

Article

Not peer-reviewed version

Longitudinal Changes in Brain Connectivity Correlate with Neuropsychological Testing in Brain Tumor Resection Patients

[David G Ellis](#) , [David Warren](#) , [Matthew Garlinghouse](#) , [Michele R Aizenberg](#) *

Posted Date: 24 October 2024

doi: 10.20944/preprints202405.0739.v2

Keywords: Brain connectivity; brain tumor; graph theory; connectome; neuropsychological evaluation



Preprints.org is a free multidiscipline platform providing preprint service that is dedicated to making early versions of research outputs permanently available and citable. Preprints posted at Preprints.org appear in Web of Science, Crossref, Google Scholar, Scilit, Europe PMC.

Copyright: This is an open access article distributed under the Creative Commons Attribution License which permits unrestricted use, distribution, and reproduction in any medium, provided the original work is properly cited.

Disclaimer/Publisher's Note: The statements, opinions, and data contained in all publications are solely those of the individual author(s) and contributor(s) and not of MDPI and/or the editor(s). MDPI and/or the editor(s) disclaim responsibility for any injury to people or property resulting from any ideas, methods, instructions, or products referred to in the content.

Article

Longitudinal Changes in Brain Connectivity Correlate with Neuropsychological Testing in Brain Tumor Resection Patients

David G. Ellis, MS,¹ Matthew Garlinghouse, PhD,² David E. Warren, PhD,³
Michele R. Aizenberg and MD¹

¹ Department of Neurosurgery, University of Nebraska Medical Center, Omaha, Nebraska, USA

² Nebraska-Western Iowa Veteran's Affairs Medical Center, Omaha, Nebraska, USA

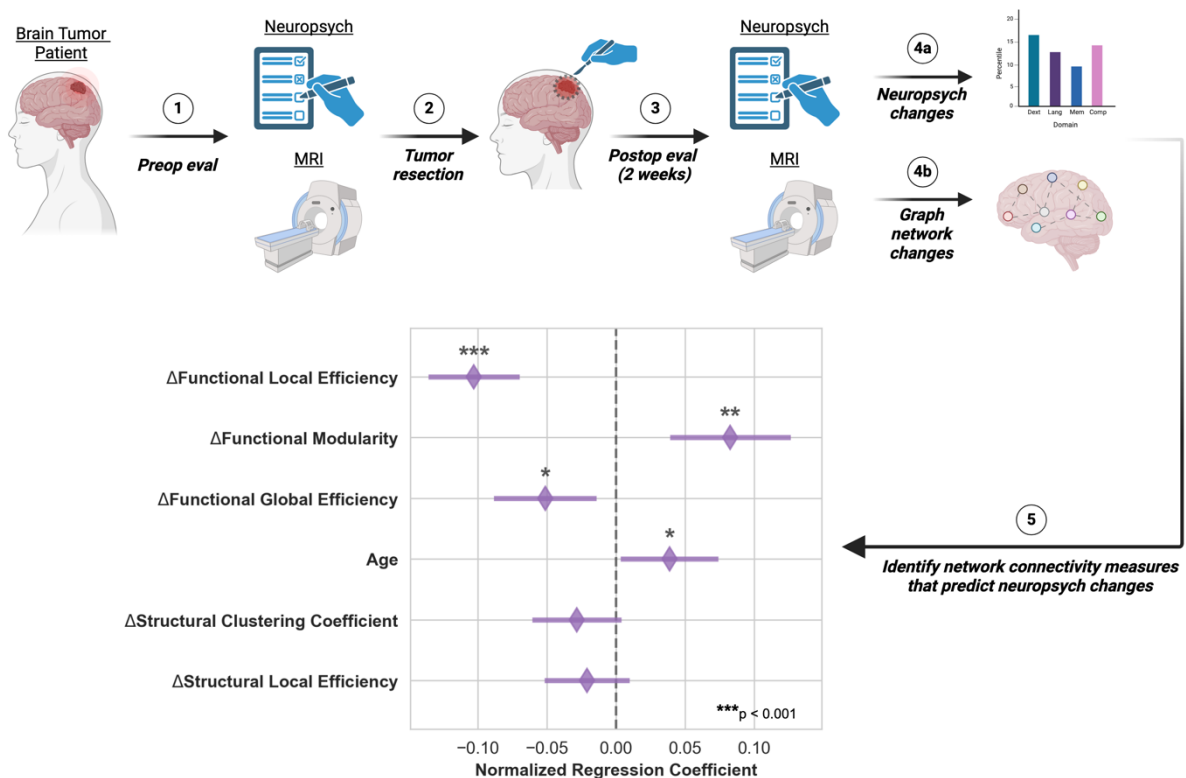
³ Department of Neurological Sciences, University of Nebraska Medical Center, Omaha, Nebraska, USA

* Correspondence: maizenberg@unmc.edu

Abstract: Background: Patients undergoing brain tumor resection experience neurological and cognitive (i.e., neurocognitive) changes reflected in altered performance on neuropsychological tests. These changes can be difficult to explain or predict. Brain connectivity, measured with neuroimaging, offers one potential model for examining these changes. In this study, we evaluated whether longitudinal changes in brain connectivity correlated with changes in neurocognitive abilities in patients before and after brain tumor resection. Methods: Patients underwent functional and diffusion MR scanning and neuropsychological evaluation before tumor resection followed by repeat scanning and evaluation two weeks post-resection. Using this functional and diffusion imaging data, we measured changes in the topology of the functional and structural networks. From the neuropsychological testing scores, we derived a composite score that described a patient's overall level of neurocognitive functioning. We then used a multiple linear regression model to test whether structural and functional connectivity measures were correlated with changes in composite scores. Results: Multiple linear regression on 21 subjects showed that connectivity changes were highly correlated with changes in neuropsychological evaluation scores (R^2 adjusted = 0.79, $p < 0.001$). Changes in functional local efficiency ($p < 0.001$) and global efficiency ($p < 0.05$) were inversely correlated with changes in composite score, while changes in modularity ($p < 0.01$) as well as the patient's age ($p < 0.05$) were directly correlated with changes in composite score. Conclusion: Short interval changes in brain connectivity markers were strongly correlated with changes in the composite neuropsychological test scores in brain tumor resection patients. Our findings support the need for further exploration of brain connectivity as a biomarker relevant to brain tumor patients.

Keywords: Brain connectivity; brain tumor; graph theory; connectome; neuropsychological evaluation

Visual Abstract



Introduction

For brain tumor patients, surgical resection can increase longevity and enhance quality of life. These benefits are maximized when neurosurgeons exercise skill to avoid highly disruptive, surgically-induced deficits by using tools such as preoperative functional imaging and intraoperative stimulation [1–3]. However, even when neurosurgeons appropriately utilize tools and expertise, many brain tumor patients still experience unexpected changes in their neurological and cognitive functioning (i.e., neurocognition) following surgery [4–6].

One potential means for exploring the relationship between changes in neurocognitive function related to observable changes in the brain could be to use brain connectivity markers derived from neuroimaging. Previous research has indicated the utility of using brain connectivity to better understand the effects of brain tumors and their treatment. For instance, functional and structural connectivity have been shown to have a significant impact on brain tumor patient outcomes [7]. Interestingly, structural connectivity helps explain glioma infiltration patterns, and the disruption of the structural connectome beyond the focal lesion has been shown to impact survival [8]. Meanwhile, functional connectivity has been shown to be altered in regions both proximal and distal to gliomas, and the quantity of these abnormal connections relates to tumor aggressiveness and cognitive function [9]. Furthermore, pre-surgical functional connectivity has been shown to have utility for predicting patient survival and functional status [10,11].

While brain connectivity has proven useful in understanding the effects of tumors on brain function, it has not yet been shown whether longitudinal changes in connectivity correlate to changes in neurocognition. Understanding the relationship between connectivity and neurocognition could inform the discovery of biomarkers that are relevant for non-invasive patient monitoring and surgical planning. To this end, we examined the relationship between graph network connectivity and

neuropsychological measures in patients before and after tumor resection surgery and identified key connectivity markers predictive of cognitive and neurological changes.

Methods

Subject Enrollment and Clinical Care

For this pilot study, adult patients (≥ 19 years old in Nebraska) were considered for enrollment if they had a supratentorial primary or metastatic tumor or cavernoma for which resective surgery was recommended. Subjects could not have had any prior brain treatments (surgery, radiation) or a history of a neurodegenerative disorder. After consent and enrollment, patients had preoperative clinical, neuropsychological, quality of life, and imaging (MRI) evaluations within one week prior to surgery. Tumor resection was performed via craniotomy for resection of their lesion, and the patients received standard perioperative clinical care. Two weeks postoperatively, clinical, neuropsychological, quality of life, and imaging studies were repeated. Healthy control subjects were also enrolled to evaluate the effect of repeat testing. For control subjects, no surgery was performed, but the same neuropsychological, quality of life, and imaging assessments were performed two weeks apart.

Neuropsychological Testing

Subjects and controls were administered neuropsychological evaluations and quality of life (QOL) inventories (Table S1). This test battery was designed to assess cognitive and neurological functions commonly noted in the literature to be compromised in patients with gliomas [12–14]. Testing domains consisted of basic attention, dexterity, executive, language, memory, and speeded processing. See supplementary material for more details.

To assess the patient's abilities within a given domain (listed in Table S1), the reported percentile scores of the tests within each domain were averaged, similar to previous studies [12,15,16]. We computed a single clinical trial battery composite (CTB Comp) score per subject from the averaged domain scores. We used this score to assess the overall combined changes in neurocognitive functioning and impairment per subject.

Image Acquisition

In addition to our standard clinical brain tumor MRI protocol at the timepoints mentioned above, we acquired research sequences consisting of high angular resolution diffusion MRI (dMRI) and 26 minutes of high-resolution resting-state functional MRI (rs-fMRI) according to the protocol from the Human Connectome Project on Development and Aging (HCP D/A) [17]. We used the Siemens Prisma 3T MR scanner at the University of Nebraska Medical Center Core for Advanced Magnetic Resonance Imaging Facility (RRID:SCR_022468) for all scanning sessions. The HCP D/A designed the protocol for the Siemens Prisma scanner to optimize data quality and efficiency for developing and aging cohorts [17]. This protocol allows for high resolution, 1.5mm and 2mm isotropic for dMRI and rs-fMRI, respectively. We acquired the dMRI data with two shells, 1500 and 3000 s/mm^2 , with 92-93 directions per shell, each acquired twice in opposite phase encoding directions and 28 b0 volumes interspersed equally. In addition, we acquired a total of 1952 rs-fMRI volumes over four runs for a total of about 26 minutes of rs-fMRI data. Acquiring a large number of volumes over multiple runs has been shown to provide enhanced results for mapping functional connectivity in individual subjects [18,19].

Image Processing

We performed image processing using an in-house processing pipeline written utilizing NiPype [20] and incorporating processing workflows from fMRIPrep [21] and related projects [22]. We designed the in-house pipeline to allow for enhanced customizability of the image registrations and transformations not offered in fMRIPrep. The node definitions were defined by the Schaefer et al. 300

parcellation seven-network atlas [23] in FSL's asymmetric MNI space [24] as acquired from TemplateFlow [25]. To account for any distortions caused by surgery or tumor growth, the registrations between the preoperative and postoperative T1w scans for an individual patient were computed using non-linear registrations. All non-linear registrations were performed using the Advanced Normalization Tools (ANTs) SyN registration algorithm [26].

Functional Image Processing

Head motion correction [27] and susceptibility distortion correction [28] were performed on the rs-fMRI using FSL [29] and fMRIPrep [21]. The alignment between each rs-fMRI scan and the T1w image for that scanning visit was computed using a boundary-based rigid registration in FreeSurfer [30]. Transformation into MNI space through preoperative T1w space was performed in a single step that included head motion and susceptibility distortion correction transforms. Due to the TR being much shorter than standard fMRI sequences (TR=770ms for the rs-fMRI scans compared to a TR of about 2.5s for a standard fMRI scan), we did not perform slice timing correction, which is the same approach used by the HCP for their processing pipelines [31]. To correct for artifacts in the BOLD acquisition, we adopted the Power et al. approach to denoising by simultaneously applying high-pass and low-pass filters, regressing out of 24 motion regressors along with global signal, and censoring of high motion timepoints [32]. Any timepoints with less than five minutes of resting state data following denoising were excluded from the analysis.

Following preprocessing, the whole brain functional networks were constructed with Nilearn [33]. The regions of interest from the Schaefer et al. parcellation atlas [23] were used as the nodes of the network [34,35], with the connections between nodes being defined as the temporal correlation between the regions of interest. To allow consistent comparison between timepoints, the networks were normalized to only include the connections with correlations at or above the 80th percentile (i.e., the network density was set at 20%).

Diffusion Image Processing

The diffusion imaging data were processed in the native diffusion space. The alignment between the diffusion imaging and the T1w image for that scanning visit was computed using a rigid registration. Head motion correction [27], susceptibility distortion correction [28], and eddy current correction [29,36]. Multi-shell multi-tissue constrained spherical deconvolution was used to estimate fiber orientation distributions [37]. Next, anatomically constrained tractography (ACT) was performed to generate white matter tracts for each subject and session [38]. This method of tractography limits the white matter tracts to terminate mainly at the boundary between the gray matter and the white matter or within the deep gray. Constraining the tractography in this way makes the assignment of tracts to cortical regions straightforward. Finally, we applied spherical deconvolution-informed filtering of tractograms (SIFT) to the white matter tracts to filter out tracts less likely to be accurate [39]. We then constructed the structural connectome matrix by counting the number of estimated white matter tracts between any two brain regions as defined by the Harvard-Oxford atlas transformed through the preoperative T1w space into the native diffusion space [40]. Two nodes of the atlas were determined to be connected if five or more reconstructed tracts connect those regions. This overall method of reconstructing white matter tracts increases the accuracy of the tractography results [41] and has been used previously to estimate the structural connectome in brain tumor patients [34].

Graph Network Measures

With both the functional and structural networks constructed, we computed graph network measures for all scanning visits. We focused on whole-brain network measures rather than individual nodes or connections due to the variability in the location of the tumors, tumor-induced brain disruptions, and surgical treatment. We focused on the following network measures that have shown

promise in previous brain imaging studies: modularity, clustering coefficient, and global/local efficiency.

Modularity measures how well networks can be divided into modules. A module is a subset of nodes that are more densely connected to each other than to the rest of the network. A network with higher modularity will have modules containing nodes that are more closely connected to each other and more loosely connected to the nodes of other modules [42,43]. Similarly, the clustering coefficient is a measure of the degree to which brain regions in the network tend to form tightly interconnected clusters or communities. Modularity of the functional brain network has been shown to be increased in early-onset multiple sclerosis (MS) patients and correlated negatively with task performance in those patients [44]. The modularity of the functional network has also been shown to change in the brains of subjects undergoing sleep deprivation as well as those recovering from stroke [45,46]. To compute the modularity of the brain networks, we assigned each node to a module based on the network assigned by Yeo et al. 7-network atlas (visual, somatomotor, dorsal attention, ventral attention, limbic, frontoparietal, and default mode) [23,47].

In addition to modularity and clustering coefficient, we also measured the global efficiency (i.e., the efficiency of the parallel information transfer in the network) as well as the mean local efficiency across all nodes (i.e., the fault tolerance of the network) [48]. All graph network connectivity measures were computed using the Brain Connectivity Toolbox for Python (<https://pypi.org/project/bctpy/>) [49].

In Figure 1, we show some examples of simple graph networks and how connections between and within modules change the network measures. Figure 1B shows that adding intra-module connections to the simple network, shown in Figure 1A, increases the clustering coefficient by making the modules form tighter network clusters and local efficiency by making the neighbors of many of the nodes more fault tolerant to loss of any given node. Figure 1C shows that adding inter-module connections decreases the modularity of the network by making each of the modules less segregated. Figure 1D shows that adding both inter- and intra-module connections produces a combination of decreased modularity with increased efficiency and clustering coefficient.

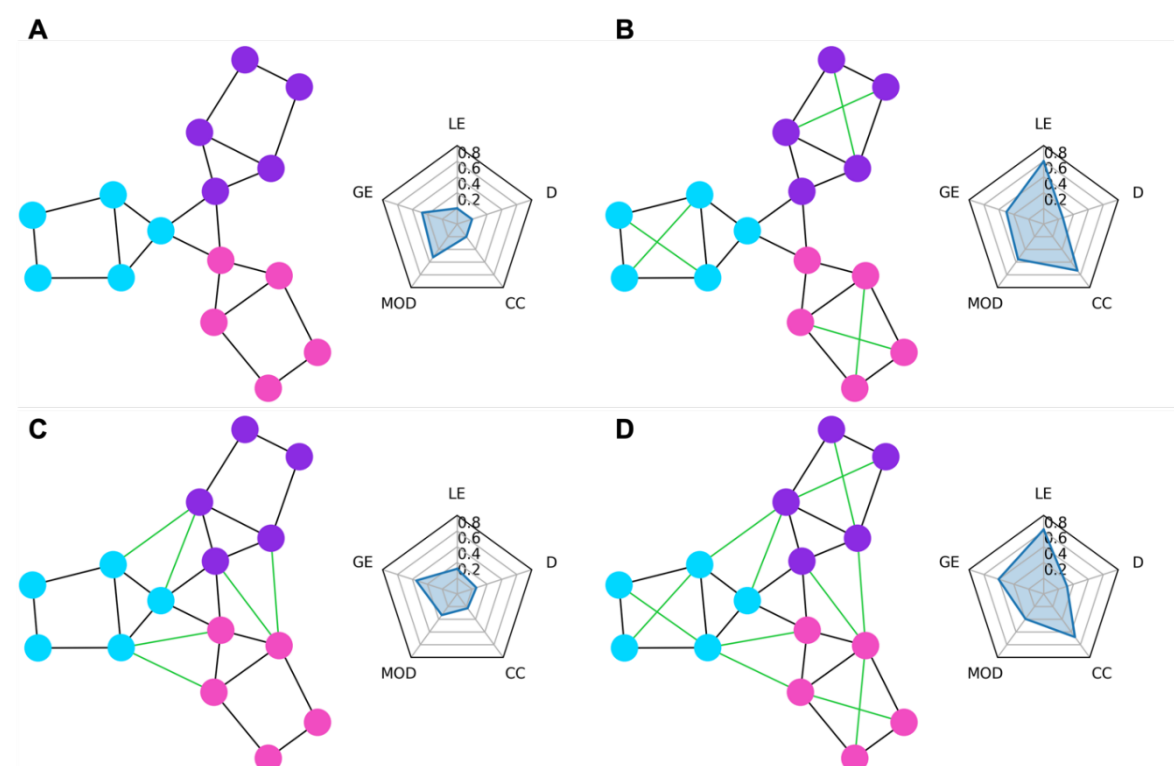


Figure 1. Example graph networks and corresponding graph theory measures shown in radar charts. The circles represent the nodes of the network while the lines represent the edges. Each node belongs to either the purple, blue, or pink module. The radar chart to the

right of each network shows the graph theory measures of local efficiency (LE), global efficiency (GE), modularity (MOD), clustering coefficient (CC), and density (D) for that network. (A) shows a simple network with three distinct modules. (B) shows the network from A but with added connections (green edges) within each module. These within-module connections greatly increase the local efficiency (local fault tolerance) and clustering coefficient and slightly increase the modularity and global efficiency. (C) shows the network from A but with added connections between modules which decrease modularity but provide a small increase to local efficiency. (D) shows the network from A but with both the within module connections from B and between module connections from C added. Compared to B, the modularity is decreased due to the between module connections, while compared to C the local efficiency, global efficiency, and clustering coefficient are all increased due to the added within module connections.

Statistical Analysis

To evaluate the relationship between brain connectivity measures and changes in neuropsychological assessments, we fitted a multiple regression linear model. We used both the structural and functional connectivity changes along with the demographic variables of sex and age as the predictor variables and the composite score changes as the response variable. Before fitting the model, we first removed redundant predictors by removing variables that had a Pearson correlation of absolute value greater than 0.8 to other predictors. We then performed feature selection using LASSO linear regression using glmnet in R [50,51]. The selected features from the LASSO regression were used as the predictor variables to the multiple regression model evaluating the relationship between the predictors and the composite score changes.

Results

Enrollment

We enrolled a total of 38 patients, 21 of whom had complete sets of neuropsychological testing and MRI (Supplementary Table S1). As shown in Table 1, the average age at the time of surgery was 50.8 years (SD=11.8). Table 2 shows the distribution of tumor diagnosis and tumor location: 51% of the cases were either high- or low-grade gliomas, and the cases were almost evenly split between the right (51%) and left (49%) hemispheres. After censoring timepoints affected by motion, each scanning session contained 12-26 minutes of resting state fMRI data (mean=23.7 minutes, standard deviation=4.2 minutes). The average number of days between scanning sessions was 18.2 days for patients and 18.7 for controls. To evaluate the effect of repeat testing, seven healthy control subjects were also enrolled, with 6 completing all evaluations. While the demographics of the control group were substantially different from that of the patient group in terms of age and education, the use of the control data was limited to the evaluation of changes in test scores following surgery and did not affect any of the other analyses.

Changes in Neuropsychological Test Scores Following Surgery

The domain scores for Quality of Life, Dexterity, and Memory improved in patients postoperatively ($p < 0.05$), but these changes were not significantly different from the controls (Figure 2). The control group had a significant increase in the Memory domain scores ($p < 0.05$) but not for any of the other domains. Because none of the neuropsychological domain score changes for the patient group were different from the controls, we could not conclude that the neuropsychological domain scores changed because of surgery or tumor removal. Further analysis on the subset of patients that had gliomas showed that these patients followed the same trends as that of the entire cohort and had significant increases in memory and dexterity scores following surgery.

Table 1 - *Subject Demographics.*

	Patients (n=37)	Controls (n=6)
Age (years)		
Mean (±SD)	50.1 (±11.8)	32.8 (±3.8)
Range	26 – 71	27 – 37
Handedness		
R (%)	33 (89%)	6 (100%)
L (%)	4 (11%)	0 (0%)
Education (years)		
Mean (±SD)	13.8 (±2.3)	19.2 (±1.8)
Range	11 – 18	16 – 21
Sex		
M (%)	24 (65%)	3 (50%)
F (%)	13 (35%)	3 (50%)

Table 2 - *Patients’ tumor characteristics.*

	Count (%)
Classification	
LGG	5 (14%)
HGG	14 (38%)
Met	11 (30%)
Meningioma	4 (11%)
Cavernoma	3 (8%)
Hemisphere	
R	18 (49%)
L	19 (51%)
Location	
Frontal	10 (27%)
Frontoparietal	1 (3%)
Occipital	4 (11%)
Parietal	9 (24%)
Temporal	11 (30%)
Frontal/Cingulate	1 (3%)
Insula	1 (3%)

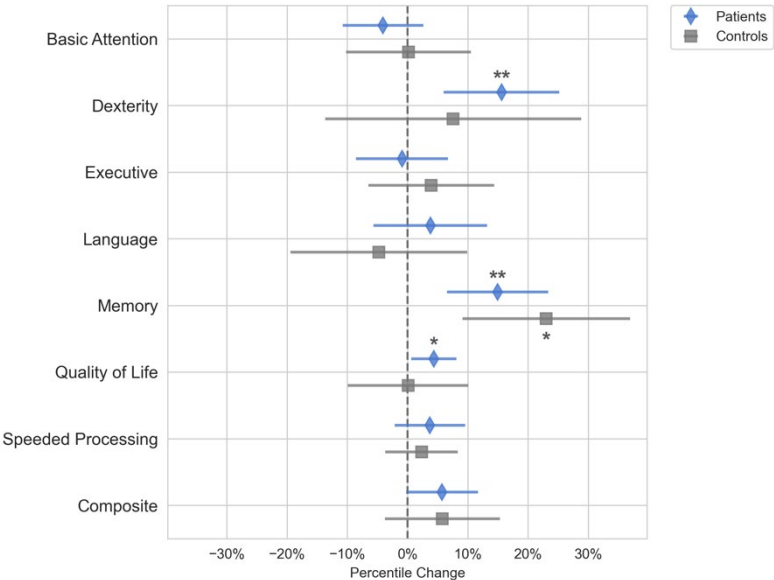


Figure 2. Changes in composite scores in brain tumor patients after tumor resection (blue diamond). Quality of Life improved post-surgery (p<0.05), as did Dexterity, and Memory scores (p<0.005). However, these changes were not significantly different than those in the control group of healthy subjects that did not have surgery (light gray square). Therefore, the improvements in Dexterity and Memory are potentially the result of practice increasing both the control and patient scores rather than surgery which would only increase the

patient scores. All other cognitive domain scores did not statistically change from baseline in either the tumor or control cohort. (* $p < 0.05$, ** $p < 0.01$).

Feature Selection

We removed the changes in mean functional clustering coefficient from the analysis because it strongly correlated with changes in functional global efficiency, with Pearson $r = -0.91$ (Figure S1). All features were z-score normalized and LASSO regression was used to select the best features. The LASSO regularization weight was optimized using 10-fold cross validation. The regularization weight resulting in the lowest validation mean-squared error, which corresponded to validation $R^2=0.55$, was used to train a final LASSO model to choose the best predictor variables. This model eliminated sex, structural modularity, and structural global efficiency from the analysis. The remaining six features were used to fit a multiple regression model without regularization on the 21 patients with complete neuropsychological testing and MRI.

Multiple Linear Regression Analysis

The multiple regression model showed that changes in connectivity was highly correlated with changes in the neuropsychological composite scores ($R^2=0.85$, R^2 adjusted=0.79, F-statistic=13.4, $p<0.001$). Changes in functional local efficiency ($p<0.001$), functional modularity ($p<0.01$), and functional global efficiency ($p<0.05$) as well as the patient's age ($p<0.05$) were significantly correlated with changes in composite neuropsychological score, as shown in Figure 3. Functional local efficiency and modularity demonstrated the strongest associations with composite score, and these associations were maintained when examining only the subset of patients with gliomas (Figure 3). Specifically, functional local efficiency was inversely correlated with composite score while functional modularity was directly correlated.

We also fitted additional multiple linear regression models with each of the domain scores as the outcome variable to assess if the relationship between connectivity varied by domain. As shown in Figure S2, we found that the relationship between the domain scores and the connectivity variables followed the same trend as that of the main model.

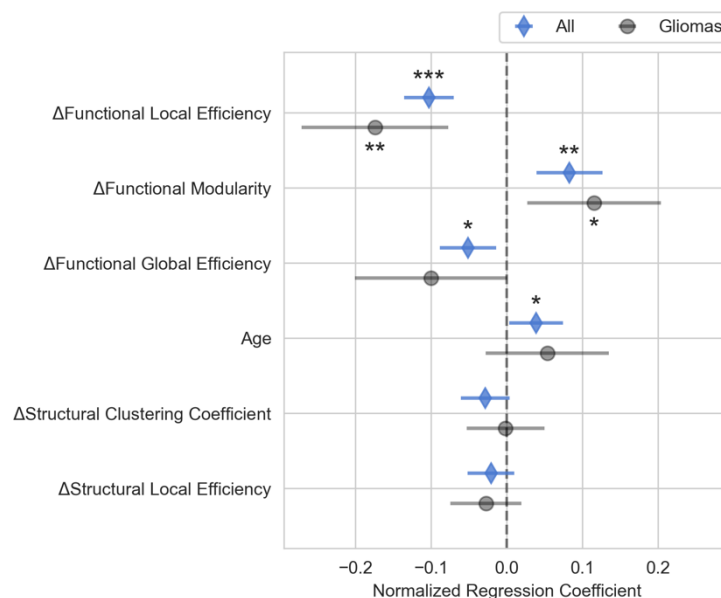


Figure 3. Relationship between changes in composite neuropsychological test scores and in brain connectivity. This figure shows the normalized regression estimates (sorted by p value) and 95% confidence intervals of the multiple linear regression model predicting changes in the composite neuropsychological score for all patients (blue diamond) as well as the subset of glioma patients (gray circles). Changes in functional local and global

efficiency were inversely correlated with changes in composite score while changes in functional modularity and age were directly correlated with changes composite score. The gliomas subset shows that the relationship between connectivity markers and composite score for patients with infiltrative tumors is similar to that of the whole cohort. (* $p < 0.05$, ** $p < 0.01$, *** $p < 0.001$).

Discussion

This study shows that changes in functional brain network connectivity were highly correlated with neuropsychologic measure changes in brain tumor resection patients. Specifically, our model revealed a strong relationship between neuropsychological test score changes and changes in the functional brain connectivity measures of local and global efficiency as well as modularity.

The finding that functional modularity was directly correlated with neuropsychological measures corroborates previous studies showing functional modularity to be a biomarker associated with improved cognitive functioning [46,52–54]. For instance, Siegel et al. found significantly increased functional modularity at three months post-stroke in patients with good recovery from language, spatial memory, and attention deficits [46].

The strong inverse relationship between changes in mean functional local efficiency and neuropsychological testing scores suggests that increasing functional local efficiency may have negative effects on neurocognitive functioning in brain tumor patients. Other research studies have found functional local efficiency to be negatively correlated with cognitive performance [55–57]. In a study of 29 healthy adults, Stanley et al. found that functional local efficiency during working memory tasks was inversely correlated to working memory performance [55]. This finding supports the role of decreased local efficiency correlating to better cognitive performance. Interestingly, Stanley et al. only found the local efficiency to be predictive of working memory performance during task performance and not while the subject was at rest [55], while our results show that the changes to the local efficiency at rest are highly predictive of overall changes to neuropsychological measures. Also supporting the inverse role of functional local efficiency in cognitive performance, Kawagoe et al. performed a cross-sectional study in elderly individuals and found that higher functional local efficiency at rest correlated to lower executive function performance and worse physical fitness [56]. While it is not clear as to why better functional local efficiency would negatively affect neurocognitive functioning, one explanation could be that increased hyper-local integration is a sign of adaptation to surgical insult. We hope that future research will further elucidate how the brain connectivity of tumor patients relates to their neurocognitive functioning.

While functional connectivity measures correlated to changes in composite score, we did not see an overall change in the composite neuropsychological score following surgery relative to the controls. Dexterity and memory functioning scores improved; however, these improvements were not significantly different from the control group. Because both controls and patients improved in their performance on these assessments, it is likely that the improvement in these domains represents the improvement due to practice effects rather than surgical treatment. Quality of life metrics improved postoperatively in the surgery group, indicating that tumor resection had a positive impact on patients' well-being.

Limitations

Our results serve as a preliminary analysis to test the utility of brain connectivity markers to explain changes in neuropsychological test scores and to identify key connectivity measures most predictive of neurocognitive outcomes in brain tumor resection patients. A crucial next step is to validate the predictive ability of these brain connectivity measures in an independent cohort of patients in a longitudinal study.

We modeled the brain connectivity measures together in a single multiple linear regression model rather than in separate models. Combining the connectivity measures into a single model is intuitive, as brain connectivity is complex and unlikely to be convincingly captured by a single metric. This approach, however, requires that the interpretation of the effects of a single brain connectivity

metric be made with caution. The coefficients associated with each connectivity measure in the model represent the relationship between that specific measure and the changes in neuropsychological test scores while holding all other variables constant. In situ, however, brain connectivity measures do not change in isolation, and inferences about changes in neurocognitive scores can only be made when accounting for the changes in all the variables.

We observed low compliance from our patients for the neuropsychological testing, likely due to the mental demands of the neuropsychological evaluations under already stressful circumstances for the patients[58]. Interestingly, compliance with MR scanning was much higher, indicating that, if robust and replicable associations are found, brain connectivity markers could be a less burdensome means of tracking cognitive and neurological functioning.

Even when patients with significant impairments complied with testing, many of the tests were not sensitive enough to measure changes in states of impairment. For example, an elderly patient in our study presented with language deficits and poor overall neurocognitive functioning. This patient was unable to complete most of the assessments both preoperatively and postoperatively preventing us from tracking any postoperative changes from baseline. However, upon clinical assessment, the physician (author MA) noted an improvement in their functioning. Therefore, this patient group may be better monitored with neuropsychological measurement tools that can detect changes in the levels of impairment without being overly burdensome.

Another factor may be timing. These assessments were conducted only two weeks apart, and it may be that the neuropsychological testing changes are transient and lack clinical relevance. In the postoperative period, patients experience the effects of medications, brain shift, physical fatigue, sleep deprivation, and other factors that may affect brain function. The amount of time necessary for the resolution of these changes and their effects is unknown. We selected our time interval for testing to isolate surgical effects as well as minimize perioperative medication effects.

Conclusions

We found that short interval changes in brain connectivity markers were highly correlated with changes in the composite neuropsychological test scores. Our findings support the need for further exploration of brain connectivity as a biomarker relevant to the neurocognitive status of brain tumor resection patients. After further validation, brain connectivity markers might aid in tracking the effects of treatment on patient cognitive functioning, potentially reducing reliance on neuropsychological testing. Future research could also explore using anticipated changes in brain network topology to better inform surgical approaches. By modeling brain networks resulting from different tumor resection strategies prior to surgery, it may be possible to identify approaches that optimize brain network characteristics and improve patient outcomes. Furthermore, future research could also explore changes in brain connectivity that result from tumor interactions with neurons. Nonetheless, further research is needed to better understand how surgical and other interventions affect brain networks and how network changes impact neurocognitive outcomes.

Disclosures: The project described is supported by the National Institute of General Medical Sciences, U54 GM115458, which funds the Great Plains IDeA-CTR Network. It was awarded to author MA. The content is solely the responsibility of the authors and does not necessarily represent the official views of the NIH.

Acknowledgments: Thank you to Jill Skorupa, RN, BSN, Katie Burcal, MS, Dulce Maroni, PhD, and James Brown, BS, for assisting with data collection and coordinating enrollment. Visual abstract was created with BioRender.com.

Describe any perceived Conflict(s) of Interest: All authors declare no conflicts of interest.

References

1. Luna, L.P.; Sherbaf, F.G.; Sair, H.I.; Mukherjee, D.; Oliveira, I.B.; Köhler, C.A. Can Preoperative Mapping with Functional MRI Reduce Morbidity in Brain Tumor Resection? A Systematic Review and Meta-Analysis of 68 Observational Studies. *Radiology* **2021**, *300*, 338-349. <https://doi.org/10.1148/radiol.2021204723>.

2. Hamer, P.D.W.; Robles, S.G.; Zwinderman, A.H.; Duffau, H.; Berger, M.S. Impact of intraoperative stimulation brain mapping on glioma surgery outcome: A meta-analysis. *J. Clin. Oncol.* **2012**, *30*, 2559-2565.
3. Ellis, D.G.; White, M.L.; Hayasaka, S.; Warren, D.E.; Wilson, T.W.; Aizenberg, M.R. Accuracy analysis of fMRI and MEG activations determined by intraoperative mapping. *Neurosurg. Focus* **2020**, *48*, E13.
4. Lacroix, M.; Abi-Said, D.; Fourney, D.R.; Gokaslan, Z.L.; Shi, W.; DeMonte, F.; Lang, F.F.; McCutcheon, I.E.; Hassenbusch, S.J.; Holland, E.; et al. A multivariate analysis of 416 patients with glioblastoma multiforme: Prognosis, extent of resection, and survival. *J. Neurosurg.* **2001**, *95*, 190-198. <https://doi.org/10.3171/jns.2001.95.2.0190>.
5. Gulati, S.; Jakola, A.S.; Nerland, U.S.; Weber, C.; Solheim, O. The Risk of Getting Worse: Surgically Acquired Deficits, Perioperative Complications, and Functional Outcomes After Primary Resection of Glioblastoma. *World Neurosurg.* **2011**, *76*, 572-579. <https://doi.org/>.
6. Jakola, A.S.; Unsgård, G.; Solheim, O. Quality of life in patients with intracranial gliomas: The impact of modern image-guided surgery: Clinical article. *Journal of Neurosurgery JNS* **2011**, *114*, 1622-1630. <https://doi.org/>.
7. Salvalaggio, A.; Pini, L.; Bertoldo, A.; Corbetta, M. Glioblastoma and brain connectivity: The need for a paradigm shift. *The Lancet Neurology* **2024**, *23*, 740-748. [https://doi.org/10.1016/S1474-4422\(24\)00160-1](https://doi.org/10.1016/S1474-4422(24)00160-1).
8. Wei, Y.; Li, C.; Cui, Z.; Mayrand, R.C.; Zou, J.; Wong, A.L.K.C.; Sinha, R.; Matys, T.; Schönlieb, C.-B.; Price, S.J. Structural connectome quantifies tumour invasion and predicts survival in glioblastoma patients. *Brain* **2023**, *146*, 1714-1727. <https://doi.org/10.1093/brain/awac360>.
9. Stoecklein, V.M.; Stoecklein, S.; Galiè, F.; Ren, J.; Schmutzer, M.; Unterrainer, M.; Albert, N.L.; Kreth, F.-W.; Thon, N.; Liebig, T.; et al. Resting-state fMRI detects alterations in whole brain connectivity related to tumor biology in glioma patients. *Neuro Oncol.* **2020**. <https://doi.org/10.1093/neuonc/noaa044>.
10. Luckett, P.H.; Olufawo, M.O.; Park, K.Y.; Lamichhane, B.; Dierker, D.; Verastegui, G.T.; Lee, J.J.; Yang, P.; Kim, A.; Butt, O.H.; et al. Predicting post-surgical functional status in high-grade glioma with resting state fMRI and machine learning. *J. Neurooncol.* **2024**. <https://doi.org/10.1007/s11060-024-04715-1>.
11. Luckett, P.H.; Park, K.Y.; Lee, J.J.; Lenze, E.J.; Wetherell, J.L.; Eyler, L.T.; Snyder, A.Z.; Ances, B.M.; Shimony, J.S.; Leuthardt, E.C. Data-efficient resting-state functional magnetic resonance imaging brain mapping with deep learning. *J. Neurosurg.* **2023**, 1-12. <https://doi.org/10.3171/2023.3.Jns2314>.
12. Johnson, D.R.; Sawyer, A.M.; Meyers, C.A.; O'Neill, B.P.; Wefel, J.S. Early measures of cognitive function predict survival in patients with newly diagnosed glioblastoma. *Neuro Oncol.* **2012**, *14*, 808-816.
13. Noll, K.R.; Sullaway, C.; Ziu, M.; Weinberg, J.S.; Wefel, J.S. Relationships between tumor grade and neurocognitive functioning in patients with glioma of the left temporal lobe prior to surgical resection. *Neuro Oncol.* **2015**, *17*, 580-587.
14. Wefel, J.S.; Noll, K.R.; Rao, G.; Cahill, D.P. Neurocognitive function varies by IDH1 genetic mutation status in patients with malignant glioma prior to surgical resection. *Neuro Oncol.* **2016**, *18*, 1656-1663.
15. Armstrong, T.; Wefel, J.; Wang, M.; Won, M.; Bottomley, A.; Mendoza, T.; Coens, C.; Werner-Wasik, M.; Brachman, D.; Choucair, A. Clinical utility of neurocognitive function (NCF), quality of life (QOL), and symptom assessment as prognostic factors for survival and measures of treatment effects on RTOG 0525. *J. Clin. Oncol.* **2011**, *29*, 2016-2016.
16. Wefel, J.S.; Cloughesy, T.; Zazzali, J.L.; Zheng, M.; Prados, M.; Wen, P.Y.; Mikkelsen, T.; Schiff, D.; Abrey, L.E.; Yung, W.A. Neurocognitive function in patients with recurrent glioblastoma treated with bevacizumab. *Neuro Oncol.* **2011**, *13*, 660-668.
17. Harms, M.P.; Somerville, L.H.; Ances, B.M.; Andersson, J.; Barch, D.M.; Bastiani, M.; Bookheimer, S.Y.; Brown, T.B.; Buckner, R.L.; Burgess, G.C.; et al. Extending the Human Connectome Project across ages: Imaging protocols for the Lifespan Development and Aging projects. *Neuroimage* **2018**, *183*, 972-984. <https://doi.org/>.
18. Finn, E.S.; Shen, X.; Scheinost, D.; Rosenberg, M.D.; Huang, J.; Chun, M.M.; Papademetris, X.; Constable, R.T. Functional connectome fingerprinting: Identifying individuals using patterns of brain connectivity. *Nat. Neurosci.* **2015**, *18*, 1664. <https://doi.org/10.1038/nn.4135>.
19. Pannunzi, M.; Hindriks, R.; Bettinardi, R.G.; Wenger, E.; Lisofsky, N.; Martensson, J.; Butler, O.; Filevich, E.; Becker, M.; Lochstet, M.; et al. Resting-state fMRI correlations: From link-wise unreliability to whole brain stability. *Neuroimage* **2017**, *157*, 250-262. <https://doi.org/>.
20. Esteban, O.; Markiewicz, C.; Burns, C.; Johnson, H.; Ziegler, E.; Manhães-Savio, A.; Jarecka, D.; Ellis, D.; Yvernault, B.; Hamalainen, C. nipy/nipype: 1.5. 0. *Zenodo* <https://doi.org/10.5281/zenodo.2020.596855>.
21. Esteban, O.; Markiewicz, C.J.; Blair, R.W.; Moodie, C.A.; Isik, A.I.; Erramuzpe, A.; Kent, J.D.; Goncalves, M.; DuPre, E.; Snyder, M. fMRIPrep: A robust preprocessing pipeline for functional MRI. *Nature methods* **2019**, *16*, 111-116.
22. Esteban, O.; Wright, J.; Markiewicz, C.J.; Thompson, W.H.; Goncalves, M.; Ciric, R.; Blair, R.W.; Feingold, F.; Rokem, A.; Ghosh, S. NiPreps: Enabling the division of labor in neuroimaging beyond fMRIPrep. **2019**.

23. Schaefer, A.; Kong, R.; Gordon, E.M.; Laumann, T.O.; Zuo, X.-N.; Holmes, A.J.; Eickhoff, S.B.; Yeo, B.T. Local-global parcellation of the human cerebral cortex from intrinsic functional connectivity MRI. *Cereb. Cortex* **2018**, *28*, 3095-3114.
24. Evans, A.C.; Janke, A.L.; Collins, D.L.; Baillet, S. Brain templates and atlases. *Neuroimage* **2012**, *62*, 911-922.
25. Ciric, R.; Thompson, W.H.; Lorenz, R.; Goncalves, M.; MacNicol, E.; Markiewicz, C.J.; Halchenko, Y.O.; Ghosh, S.S.; Gorgolewski, K.J.; Poldrack, R.A.; et al. TemplateFlow: FAIR-sharing of multi-scale, multi-species brain models. *bioRxiv* **2022**, 2021.2002.2010.430678. <https://doi.org/10.1101/2021.02.10.430678>.
26. Avants, B.B.; Tustison, N.; Song, G. Advanced normalization tools (ANTs). *Insight j* **2009**, *2*, 1-35.
27. Jenkinson, M.; Bannister, P.; Brady, M.; Smith, S. Improved Optimization for the Robust and Accurate Linear Registration and Motion Correction of Brain Images. *Neuroimage* **2002**, *17*, 825-841. <https://doi.org/>.
28. Andersson, J.L.R.; Skare, S.; Ashburner, J. How to correct susceptibility distortions in spin-echo echo-planar images: Application to diffusion tensor imaging. *Neuroimage* **2003**, *20*, 870-888. <https://doi.org/>.
29. Woolrich, M.W.; Jbabdi, S.; Patenaude, B.; Chappell, M.; Makni, S.; Behrens, T.; Beckmann, C.; Jenkinson, M.; Smith, S.M. Bayesian analysis of neuroimaging data in FSL. *Neuroimage* **2009**, *45*, S173-186. <https://doi.org/10.1016/j.neuroimage.2008.10.055>.
30. Greve, D.N.; Fischl, B. Accurate and robust brain image alignment using boundary-based registration. *Neuroimage* **2009**, *48*, 63-72. <https://doi.org/>.
31. Glasser, M.F.; Sotiropoulos, S.N.; Wilson, J.A.; Coalson, T.S.; Fischl, B.; Andersson, J.L.; Xu, J.; Jbabdi, S.; Webster, M.; Polimeni, J.R.; et al. The minimal preprocessing pipelines for the Human Connectome Project. *Neuroimage* **2013**, *80*, 105-124. <https://doi.org/10.1016/j.neuroimage.2013.04.127>.
32. Power, J.D.; Mitra, A.; Laumann, T.O.; Snyder, A.Z.; Schlaggar, B.L.; Petersen, S.E. Methods to detect, characterize, and remove motion artifact in resting state fMRI. *Neuroimage* **2014**, *84*, 320-341. <https://doi.org/>.
33. Abraham, A.; Pedregosa, F.; Eickenberg, M.; Gervais, P.; Mueller, A.; Kossaifi, J.; Gramfort, A.; Thirion, B.; Varoquaux, G. Machine learning for neuroimaging with scikit-learn. *Front. Neuroinform.* **2014**, *8*. <https://doi.org/10.3389/fninf.2014.00014>.
34. Aerts, H.; Schirner, M.; Jeurissen, B.; Van Roost, D.; Achten, E.; Ritter, P.; Marinazzo, D. Modeling Brain Dynamics in Brain Tumor Patients Using the Virtual Brain. *eNeuro* **2018**, *5*, ENEURO.0083-0018.2018. <https://doi.org/10.1523/ENEURO.0083-18.2018>.
35. Cheng, W.; Palaniyappan, L.; Li, M.; Kendrick, K.M.; Zhang, J.; Luo, Q.; Liu, Z.; Yu, R.; Deng, W.; Wang, Q.; et al. Voxel-based, brain-wide association study of aberrant functional connectivity in schizophrenia implicates thalamocortical circuitry. *Npj Schizophrenia* **2015**, *1*, 15016. <https://doi.org/10.1038/npjSchz.2015.16>.
36. Andersson, J.L.R.; Sotiropoulos, S.N. An integrated approach to correction for off-resonance effects and subject movement in diffusion MR imaging. *Neuroimage* **2016**, *125*, 1063-1078. <https://doi.org/10.1016/j.neuroimage.2015.10.019>.
37. Jeurissen, B.; Tournier, J.-D.; Dhollander, T.; Connelly, A.; Sijbers, J. Multi-tissue constrained spherical deconvolution for improved analysis of multi-shell diffusion MRI data. *Neuroimage* **2014**, *103*, 411-426. <https://doi.org/>.
38. Smith, R.E.; Tournier, J.-D.; Calamante, F.; Connelly, A. Anatomically-constrained tractography: Improved diffusion MRI streamlines tractography through effective use of anatomical information. *Neuroimage* **2012**, *62*, 1924-1938. <https://doi.org/>.
39. Smith, R.E.; Tournier, J.-D.; Calamante, F.; Connelly, A. SIFT: Spherical-deconvolution informed filtering of tractograms. *Neuroimage* **2013**, *67*, 298-312. <https://doi.org/>.
40. Rolls, E.T.; Joliot, M.; Tzourio-Mazoyer, N. Implementation of a new parcellation of the orbitofrontal cortex in the automated anatomical labeling atlas. *Neuroimage* **2015**, *122*, 1-5. <https://doi.org/>.
41. Jeurissen, B.; Descoteaux, M.; Mori, S.; Leemans, A. Diffusion MRI fiber tractography of the brain. *NMR Biomed.* **2019**, *32*, e3785. <https://doi.org/10.1002/nbm.3785>.
42. Newman, M.E.J. Modularity and community structure in networks. *Proceedings of the National Academy of Sciences* **2006**, *103*, 8577-8582, doi:doi:10.1073/pnas.0601602103.
43. Sun, Y.; Yin, Q.; Fang, R.; Yan, X.; Wang, Y.; Bezerianos, A.; Tang, H.; Miao, F.; Sun, J. Disrupted Functional Brain Connectivity and Its Association to Structural Connectivity in Amnesic Mild Cognitive Impairment and Alzheimer's Disease. *PLoS ONE* **2014**, *9*, e96505. <https://doi.org/10.1371/journal.pone.0096505>.
44. Gamboa, O.L.; Tagliazucchi, E.; von Wegner, F.; Jurcoane, A.; Wahl, M.; Laufs, H.; Ziemann, U. Working memory performance of early MS patients correlates inversely with modularity increases in resting state functional connectivity networks. *Neuroimage* **2014**, *94*, 385-395. <https://doi.org/>.
45. Ben Simon, E.; Maron-Katz, A.; Lahav, N.; Shamir, R.; Hendler, T. Tired and misconnected: A breakdown of brain modularity following sleep deprivation. *Hum. Brain Mapp.* **2017**, *38*, 3300-3314. <https://doi.org/10.1002/hbm.23596>.

46. Siegel, J.S.; Seitzman, B.A.; Ramsey, L.E.; Ortega, M.; Gordon, E.M.; Dosenbach, N.U.F.; Petersen, S.E.; Shulman, G.L.; Corbetta, M. Re-emergence of modular brain networks in stroke recovery. *Cortex* **2018**, *101*, 44-59. <https://doi.org/>.
47. Yeo, B.T.T.; Krienen, F.M.; Sepulcre, J.; Sabuncu, M.R.; Lashkari, D.; Hollinshead, M.; Roffman, J.L.; Smoller, J.W.; Zöllei, L.; Polimeni, J.R.; et al. The organization of the human cerebral cortex estimated by intrinsic functional connectivity. *J. Neurophysiol.* **2011**, *106*, 1125-1165. <https://doi.org/10.1152/jn.00338.2011>.
48. Latora, V.; Marchiori, M. Efficient behavior of small-world networks. *Phys. Rev. Lett.* **2001**, *87*, 198701.
49. Rubinov, M.; Sporns, O. Complex network measures of brain connectivity: Uses and interpretations. *Neuroimage* **2010**, *52*, 1059-1069. <https://doi.org/>.
50. Friedman, J.H.; Hastie, T.; Tibshirani, R. Regularization Paths for Generalized Linear Models via Coordinate Descent. *Journal of Statistical Software* **2010**, *33*, 1 - 22. <https://doi.org/10.18637/jss.v033.i01>.
51. Team, R.C. R: A language and environment for statistical computing, R Foundation for Statistical Computing: Vienna, Austria, 2022.
52. Alexander-Bloch, A.; Gogtay, N.; Meunier, D.; Birn, R.; Clasen, L.; Lalonde, F.; Lenroot, R.; Giedd, J.; Bullmore, E. Disrupted Modularity and Local Connectivity of Brain Functional Networks in Childhood-Onset Schizophrenia. *Front. Syst. Neurosci.* **2010**, *4*. <https://doi.org/10.3389/fnsys.2010.00147>.
53. Gallen, C.L.; D'Esposito, M. Brain Modularity: A Biomarker of Intervention-related Plasticity. *Trends Cogn. Sci.* **2019**, *23*, 293-304. <https://doi.org/>.
54. Jalili, M. Graph theoretical analysis of Alzheimer's disease: Discrimination of AD patients from healthy subjects. *Information Sciences* **2017**, *384*, 145-156. <https://doi.org/>.
55. Stanley, M.L.; Simpson, S.L.; Dagenbach, D.; Lyday, R.G.; Burdette, J.H.; Laurienti, P.J. Changes in brain network efficiency and working memory performance in aging. *PLoS ONE* **2015**, *10*, e0123950.
56. Kawagoe, T.; Onoda, K.; Yamaguchi, S. Associations among executive function, cardiorespiratory fitness, and brain network properties in older adults. *Sci. Rep.* **2017**, *7*, 40107.
57. Cohen, J.R.; D'Esposito, M. The Segregation and Integration of Distinct Brain Networks and Their Relationship to Cognition. *The Journal of Neuroscience* **2016**, *36*, 12083-12094. <https://doi.org/10.1523/jneurosci.2965-15.2016>.
58. Burke, S.L.; Hu, T.; Naseh, M.; Fava, N.M.; O'Driscoll, J.; Alvarez, D.; Cottler, L.B.; Duara, R. Factors influencing attrition in 35 Alzheimer's Disease Centers across the USA: A longitudinal examination of the National Alzheimer's Coordinating Center's Uniform Data Set. *Aging Clin. Exp. Res.* **2019**, *31*, 1283-1297. <https://doi.org/10.1007/s40520-018-1087-6>.

Disclaimer/Publisher's Note: The statements, opinions and data contained in all publications are solely those of the individual author(s) and contributor(s) and not of MDPI and/or the editor(s). MDPI and/or the editor(s) disclaim responsibility for any injury to people or property resulting from any ideas, methods, instructions or products referred to in the content.